Spectrochimica Acta Part A: Molecular and Biomolecular Spectroscopy 327 (2025) 125301

Contents lists available at ScienceDirect

Spectrochimica Acta Part A:
Molecular and Biomolecular Spectroscopy

journal homepage: www.journals.elsevier.com/spectrochimica-acta-part-a-molecular-and-biomolecular-spectroscopy

Aggressiveness evaluation of borderline serous ovarian tumors by analysis of Psammoma bodies present in cancer tissues using micro-FTIR spectroscopy

Monica Orsini [a,*], Francesco Porcelli [b], Antonella Bianchi [c], Martina Verri [c], Serena De Santis [a], Giovanni Sotgiu [a], Susanna Romano [a], Anna Crescenzi [d]

[a] Department of Industrial, Electronic and Mechanical Engineering, Roma Tre University, Via Vito Volterra 62, 00146 Rome, Italy
[b] Istituto di Struttura della Materia - National Research Council (ISM-CNR), Area della Ricerca di Roma 1, Via Salaria km 29.300, 00015 Monterotondo, Italy
[c] Pathology Unit, Fondazione Policlinico Universitario Campus Bio-Medico, Rome, Italy
[d] Department of Radiological, Oncolological and Pathological Sciences, Sapienza University of Rome, Italy

HIGHLIGHTS

- Evaluation of borderline epithelial ovarian tumor aggressiveness is investigated.
- IR analysis of psammoma bodies present in tumor of different grade was carried out.
- Differences and similarities in the chemical content were evaluated.
- The level of carbonate content in psammoma bodies of different tumors is compared.

GRAPHICAL ABSTRACT

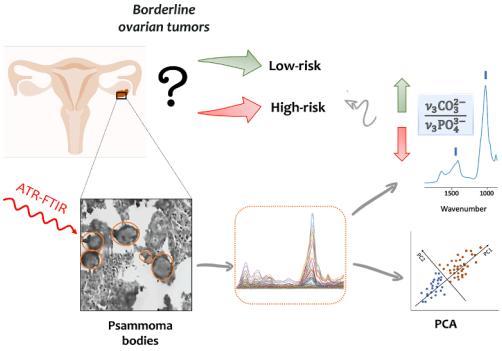

ARTICLE INFO

Keywords:
Borderline ovarian tumor
Psammoma bodies
micro-FTIR spectroscopy
Carbonate content
High-risk tumor

ABSTRACT

Borderline ovarian tumor is a type of tumor with generally low malignant potential. However, these tumors pose diagnostic challenges with benign and malignant epithelial ovarian tumors because the clinical symptoms are similar and investigation procedures for specific diagnosis are still debated. In addition, a small number of borderlines transform into high-grade serous ovarian carcinoma with a poor prognosis. Therefore, tools improving a better characterization of high-risk subtypes of borderline tumors to enable understanding of possible unfavorable evolution are essential for patients' management. Psammoma bodies (PBs) are micro-calcifications found both in serous epithelial ovarian cancer and serous borderline tumors with possible correlation with disease progression.

In this work, the chemical composition of PBs found in the tissues of borderline, high-grade and low-grade ovarian tumors was evaluated using micro-FTIR spectroscopy. Applying principal component analysis to spectral data, it was observed that among the borderline tumors analyzed (**1-bl**, **2-bl** and **3-bl**), the PBs of **3-bl** showed a different chemical content from that of the PBs of the high-grade and low-grade tumors, while the

* Corresponding author.
E-mail address: monica.orsini@uniroma3.it (M. Orsini).

https://doi.org/10.1016/j.saa.2024.125301
Received 5 June 2024; Received in revised form 7 October 2024; Accepted 16 October 2024
Available online 19 October 2024

PBs of **1-bl** and **2-bl** appeared to have similar chemical content to the PBs of high- and low-grade tumors. The discriminating wavenumbers were found to be those related to carbonate CO_3^{2-} (1454, 1413 cm^{-1} and 872 cm^{-1}) and phosphate PO_4^{3-} (1018 cm^{-1} and 960 cm^{-1}) present in microcalcifications. A higher ratio between peak intensities at 1413 cm^{-1} and 1018 cm^{-1} (I_{1413}/I_{1018}) was observed in the PBs of **3-bl** compared with those of high- and low-grade ovarian carcinoma patients, which correlates with higher CO_3^{2-} content. On the other hand, the PBs of **1-bl** and **2-bl** showed a CO_3^{2-} level close to that of the PBs of high- and low-grade patients. Several studies on microcalcifications in breast carcinoma have reported that increased carbonate content is related to decreased tumor aggressiveness. Therefore, case **bl-3** appeared to be the less aggressive. The results obtained from FTIR analysis were in agreement with histopathological tumor classification and molecular analysis for BRAFV600E. The FTIR technique could become a reliable tool for identifying borderline low- and high-risk tumors.

1. Introduction

Epithelial ovarian cancer is the second most lethal gynaecological malignancy worldwide [1]. Histological classification of epithelial ovarian cancer is, in fact, particularly complex since each subtype represents a distinct disease entity with a different site of origin, pathogenesis, clinical features, and prognosis. The 2020 World Health Organization (WHO) classification recognizes at least five distinct subtypes of malignant epithelial ovarian cancer: high-grade serous carcinoma (70 % of cases), endometrioid carcinoma (10 %), clear-cell carcinoma (6 %–10 %), low-grade serous carcinoma (5 %) and mucinous carcinoma (3 %–4%), along with other rare entities [2]. Currently, there is no reliable screening method for epithelial ovarian cancer, and most women are diagnosed based on symptoms, with the majority presenting at an advanced stage [3] with radical surgery becoming the main form of treatment.

Borderline ovarian tumors are a further heterogeneous group of uncertain malignant potential that represent about 10–20 % of all epithelial tumors of the ovary. Borderline ovarian tumors mainly occur in young, healthy women of reproductive age and generally have a favorable prognosis with a high 10-year survival rate for all stages [4], suggesting conservative approaches for fertility preservation. Unfortunately, borderline ovarian tumors are not easy to distinguish from early-stage malignant ovarian carcinoma due to the similarity between the respective symptoms, especially in advanced states, and the lack of specific tumor biomarkers and imaging examinations. Moreover, the recurrence and conversion into malignant ovarian tumors observed in a small fraction of patients pose a further challenging issue for pathologists. Such complexity and its effect on treatment choice underline the importance of histological tumor typing. Beside the European Society for Medical Oncology recommendation that pathological diagnosis should be made according to the 2020 WHO classification by an expert gynecological pathologist, it may be helpful to use alternative supporting methods to achieve a more accurate assessment of disease progression. This would lead to personalized management of the disease at the same time improve therapeutic choices.

Fourier transform infrared spectroscopy (FTIR), by measuring the absorption of infrared radiation given by the intrinsic vibrations of chemical bonds in biomolecules, provides chemical identification of the tissue sample analyzed [5,6]. In addition, the combination of infrared spectroscopy with a microscope (micro-FTIR) allows obtaining spatial information on the chemical composition of the examined tissues. In fact, optical magnification permits the observation of tissue samples at the micrometer level. At the same time infrared spectroscopy provides information on the biomolecular composition of the tissue area visualized by acquiring the corresponding IR spectrum. Spectra recorded on tissue samples are generally very complex. In addition, the differences among samples under diverse pathological conditions are very slight and difficult to notice in the raw spectra. Therefore, to obtain relevant information, spectra need to be processed. By applying multivariate analysis to spectral data, insight into slight alterations in biomolecular content can be extracted and pathological conditions can be investigated [7,8].

Standard methods used to analyze ovarian tumors and ascertain grade and aggressiveness include histopathological diagnosis and imaging techniques such as computed tomography and magnetic resonance imaging. Histopathological investigation requires complex specimen preparation, uses immunohistochemical staining or labeling and often it is time-consuming and subjective. Computed tomography and magnetic resonance imaging are expensive and usually cannot diagnose tumors at an early stage. Compared with these analysis techniques, FTIR micro-spectroscopy exhibits considerable advantages. This technique requires minimal sample preparation, is nondestructive and is not time-consuming. It proved to be a very sensitive and reliable technique. In fact, by capturing small changes in the biomolecules that compose tissues, it allows detection of precancerous lesions and following the progression of cancer. It also allows both qualitative and quantitative information on components to be obtained [9–11].

Psammoma bodies (PBs) are round, laminated, microscopic calcification mainly found in serous epithelial ovarian cancer as well as in serous borderline tumors. Their nature and significance have been evaluated in various studies [12,13], anyway no correlation between biochemical analysis of these microcalcifications and ovarian tumor behavior was reported to date. In particular, a possible relationship between chemical composition and tumor progression has not yet been investigated.

In our previous work [14], we investigated the chemical composition of PBs in ovarian tumors using the FTIR technique. Based on this study, it had been determined that the PBs found in ovarian tumors are essentially composed of amorphous calcium carbonate phosphate, a substance already found in PBs present in thyroid cancer [15]. However, the chemical composition of PBs found in ovarian tumors of different grades had not been investigated.

The aim of this work was to evaluate whether there is a difference in chemical composition among PBs present in borderline serous ovarian tumors and epithelial serous ovarian tumors.

Indeed, the knowledge of this different chemical composition and the possible correlation with disease progression may be helpful for provide insight into prognosis of serous borderline ovarian tumors.

PBs found in tissues of ovarian serous tumors from patients undergoing surgery and diagnosed with different serous tumors (high and low-grade serous carcinoma and borderline tumors) were analyzed.

The incidence of borderline tumors showing PBs is 6–18 % of all borderline serous ovarian tumors [16]. Therefore, although the number of patients enrolled in this study is not large, the preliminary results obtained could point out the FTIR technique as a valuable tool to investigate the evolution of borderline tumors.

By applying principal component analysis (PCA) to the recorded FTIR spectra of microcalcifications detected on the tissue samples, the similarities and differences in the chemical content of the microcalcifications were assessed. In addition, the carbonate content in the samples was examined. The information deduced from the spectral data opened a hypothesis of a priori knowledge of the possible evolution of the borderline tumors analyzed corroborated by evaluating molecular testing for somatic BRAF V600E mutation.

2. Experimental section

2.1. Tissue collection, histopathological classification

Tissue samples were obtained from formalin-fixed paraffin-embedded samples of surgically removed ovarian tumors from 9 patients. Three patients were diagnosed with borderline serous tumors, three patients with high-grade serous carcinomas and three patients with low-grade serous carcinomas (Table 1).

AJCC TNM cancer staging manual [17] refers to the pathologic classification of a tumor. In this classification: T describes the extent of the primary tumor (in the ovary section with numbers from 1 (limited to the ovary) to 3 (peritoneal involvement)), N specifies whether the tumor has spread to the regional lymph nodes, M indicates whether the tumor has spread to other organs (metastasis).

In our cases, among patients with borderline serous tumors, histological evaluation reported respectively a pT (primary tumor) classification of pT2a (**1-bl**), pT3b (**2-bl**), and pT1a (**3-bl**). (Table 1).

2.2. FTIR analysis of tissue samples

2.2.1. Sample preparation

Two consecutive slices of 10 μm were obtained from paraffin blocks containing the tissue samples. The first slice was stained with hematoxylin and eosin (HE) for the pathological exam and used as morphological reference to identify the presence of microcalcifications (Fig. 1a). The adjacent slice was mounted on gold coated microscope slides and deparaffinized before measurements using infrared spectroscopy. The samples were deparaffinized by immersing them in three different containers of xylene and then in two different containers of absolute alcohol. Then the samples were immersed in aqueous ethanol solutions of decreasing concentration (96 %, 80 %, 70 % and 50 %). The samples were soaked in each solution for 3 min. Finally, the samples were washed with water and air-dried. (Fig. 1b).

2.2.2. Analysis of microcalcifications using micro-Fourier transform spectroscopy (micro-FTIR)

Each sample on gold coated slides was investigated by micro-Fourier-transform infrared spectroscopy (micro-FTIR). This instrument combines an infrared spectrometer to a microscope equipped with high-resolution 1/3 in. color digital camera with 1024 × 768 XGA for the collection of visual images of the sample surface. The areas with microcalcifications were selected, microscope images were captured and point-by-point randomly FTIR spectra of microcalcifications were recorded (Fig. 1c).

Table 1
Types of ovarian tumors investigated.

Tissue samples	Classification of ovarian tumors from the 9 patients enrolled in this study	
1-bl	Borderline serous tumors (3 patients)	**pT2a**[a] (Extension or implants on the uterus or fallopian tube(s) or ovaries)
2-bl		**pT3b**[a] (Macroscopic peritoneal metastasis beyond pelvis ≤2 cm with or without retroperitoneal lymph node metastasis)
3-bl		**pT1a**[a] (Tumor limited to 1 ovary (capsule intact) or fallopian tube; no tumor on ovarian or fallopian tube surface; no malignant cells in ascites or peritoneal washings)
lg	Low-grade serous carcinomas (3 patients)	
hg	High-grade serous carcinomas (3 patients)	

[a] Pathologic TNM classification.

The instrument used was a Nicolet iN10 infrared microscope (Thermo Fisher) with a Mercury-Cadmium-Telluride (MCT-A) nitrogen-cooled detector and motorized stage. Spectra were acquired in the Attenuated Total Reflection (ATR) mode using an accessory with a germanium micro-tip of 350 μm diameter. Spectra were recorded within the 4000–800 cm^{-1} range with a resolution of 8 cm^{-1}, using an aperture of 15 × 15 μm. Sixty-four (64) interferograms were averaged per spectrum and apodized using a Blackman-Harris correction. The background spectrum was collected on air and a new background acquisition was taken before the analysis of each microcalcification. The ATR crystal was cleaned with ethanol prior to the measurement of the background. Data acquisition and spectra elaboration were carried out with the OMNIC SPECTA software provided by Thermo Fisher Scientific. The number of total spectra recorded from the different tissues analyzed is 1987. Specifically, 666 spectra were acquired on the samples of the high-grade patients **hg**, 620 spectra were recorded on the samples of the low-grade patients **lg**, 263 spectra were acquired on the samples of the borderline patient **1-bl**, 238 spectra were recorded on the samples of the borderline patient **2-bl**, and 200 spectra were recorded on the samples of the borderline patient **3-bl**.

Then spectral data were converted to files (.txt) for input to Matlab software.

Raw data were filtered imposing a threshold of 0.1 on the absorbance recorded at 1018 cm^{-1}, corresponding to PO_4^{3-} (pre-processed spectra).

2.2.3. Principal component analysis (PCA)

PCA was performed on Savitzky–Golay second derivative (11-point smoothing) pre-processed spectra related to microcalcifications detected in ovarian tissues with high-grade, low-grade and borderline cancer. PCA analysis was applied to a total number of 590 spectra. Specifically, 181 spectra were obtained from the high-grade patients **hg**, 187 spectra were obtained from the low-grade patients **lg**, 101 spectra were obtained from the borderline patient **1-bl**, 83 spectra were obtained from the borderline patient **2-bl**, and 38 spectra were obtained from the borderline patient **3-bl**.

PCA is an algorithm used to derive relevant information from confusing datasets by emphasizing similarities and differences. The original data set of variables is reduced to smaller number of orthogonal variables called the principal components (PCs). In the analysis of FTIR spectra by PCA, the scores indicate the contribute of each spectrum relative to the selected principal component.

2.2.4. Boxplot

Boxplot representation of the first two principal components for spectral data of group **bl**, **bl-1d**, **bl-3d**, **lg** was performed. This method is suitable for comparing group distributions within the dataset as it visualizes the central tendency, asymmetry, and dispersion of the data, as well as highlighting outliers. In detail, it is made of a boxplot whose lower and upper limits depict the 25- and 75 %-quartile of the data, while a bar within the boxplot represents the median, i.e., the 50 %-quartile. The boxplot includes 50 % of the data points, and the whiskers range from 75 %-quartile to the maximum of the data and 25 %-quartile to the minimum of the data, respectively.

2.2.5. Average spectra and ratio CO_3^{2-}/PO_4^{3-} determination

Baseline correction was performed on the pre-processed spectra using a homemade matlab code. After that, the mean spectra of microcalcifications detected in the ovarian tissues of the three patients with high-grade tumors and the three patients with low-grade tumors were calculated. While for the borderline patients the mean spectrum was calculated for each patient.

For each spectrum belonging to every spectral data group **1-bl**, **2-bl**, **3-bl**, **lg** the ratio CO_3^{2-}/PO_4^{3-} was calculated considering the maximum absorbance value at 1413 cm^{-1} for CO_3^{2-} and at 1018 cm^{-1} for PO_4^{3-}. After that for each determined ratio group the average value was

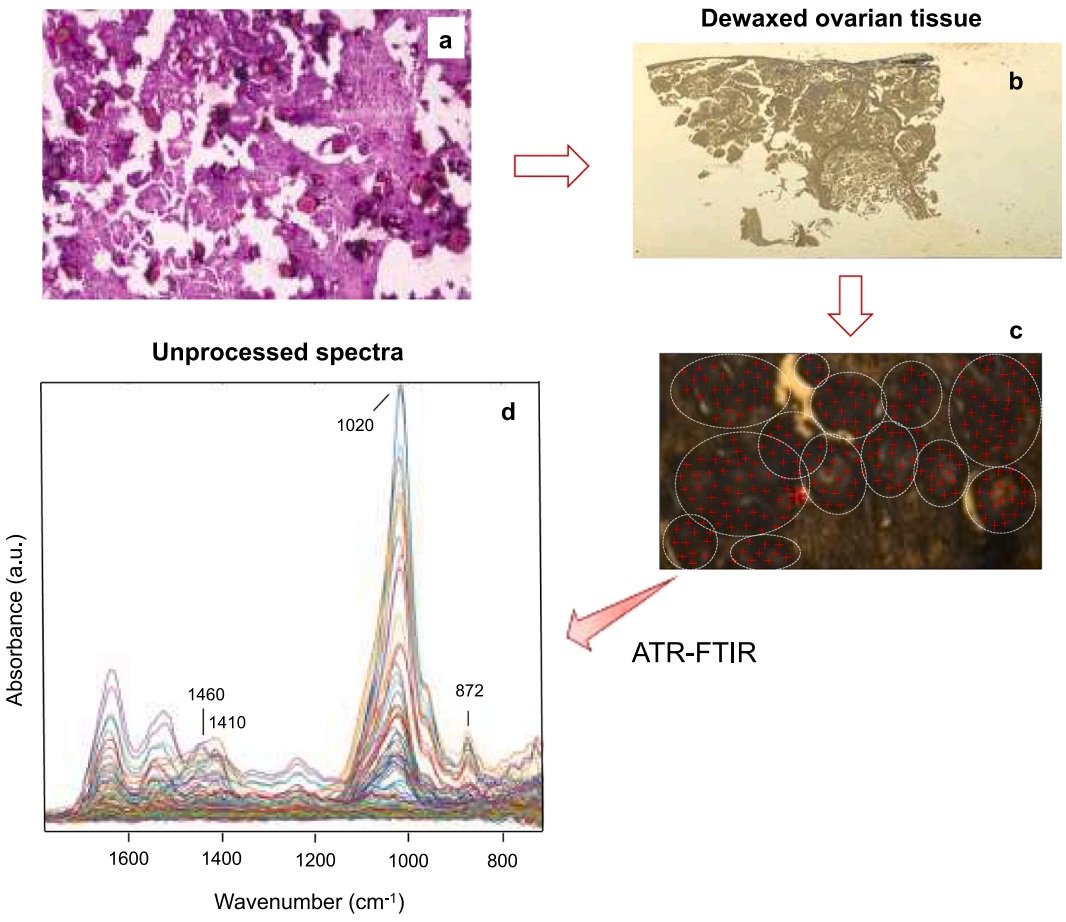

Fig. 1. (a) Histology of ovarian tissue from a serous tumor analyzed showing numerous microcalcifications (psammoma bodies), hematoxylin-Eosin stain, medium power field; (b) 10 μm thick dewaxed ovarian tissue sample on gold coated microscope slides; (c) photomicrograph obtained with the micro-FTIR digital camera of selected region of tumor tissue sample containing microcalcifications highlighted with white circles and the red marks show where the ATR-FTIR spectra were recorded; (d) the resulting unprocessed spectra.

calculated.

One-way ANOVA test was performed using pairwise comparison of the ratios CO_3^{2-}/PO_4^{3-} for the spectra of **1-bl**, **2-bl**, **3-bl**, **lg** and **hg** to assess the significance of the differences among these ratios. The threshold of statistical significance was set at $P < 0.01$ (Fig. S1).

2.3. Immunohistochemical staining for BRAF V600E mutated protein and molecular assessment for hot spot BRAF mutation status

Immunohistochemistry and molecular assessment were aimed to identify mutation of the BRAF gene that encodes the BRAF protein. This intracellular enzyme regulates physiological functions of cells, including growth, differentiation, proliferation and apoptosis. Among the possible mutations, the most common is the BRAFV600E and is caused by the substitution of glutamic acid for valine.

2.3.1. Immunohistochemistry

4-μm sections from representative paraffin blocks for each borderline case, were collected on slides and stained with hematoxylin-eosin for morphologic evaluation. After microscopic diagnosis, additional paraffin sections were cut from the blocks, collected on polarized slides, and submitted for immunohistochemical staining using an Automated stainer (Dako Omnis, Agilent). Sections were pretreated with EDTA, pH 8, and incubated with mouse anti-human BRAF(V600E) antibody, clone VE1 (Spring Bioscience, Pleasanton, CA, USA) diluted 1:50, for 30 min. This antibody recognizes the BRAF V600E mutated protein. The reaction product was revealed by peroxidase. Cases were reported as positive when a definite brown granular reaction product was seen within the cytoplasm of neoplastic cells, in the absence of background staining. Control study was performed by omitting the primary antibody. The immunostained slides were evaluated in blind by 2 expert pathologists (AC, AB), unaware of the clinico-pathologic and genetic data.

2.3.2. Molecular analysis

BRAF molecular testing was performed to confirm positive immunostaining for BRAFV600E mutations. Eight 5 μm thick sections were cut from paraffin block, dewaxed, hydrated and submitted for DNA extraction using the Qiagen mini kit. Molecular analysis was performed using PCR method in another Institution.

This study did not require ethical approval since it was retrospective and was performed using anonymized paraffin sections. The study ID was only related to the TNM stage at diagnosis. No personal data from patients were collected or shared. All the activities of the study were conducted in accordance with the 1964 Helsinki Declaration and later amendments.

3. Results and discussion

Tissue samples from patients affected by high and low-grade serous carcinoma and borderline tumors (Table 1), ascertained through histopathological classification of expert pathologist, were analyzed using ATR-FTIR microspectroscopy. After identifying the presence of microcalcifications (Fig. 1a) for each tissue sample, the successive dewaxed tissue slice, deposited on the gold slide (Fig. 1b), was examined using the

FTIR microscope. Spectra were acquired in ATR mode at several random points within the selected specific areas associated with micro-calcifications (Fig. 1c). Photomicrographs of the other tissue samples analyzed were reported in SI (Fig. S2). Microcalcifications were mainly composed of amorphous calcium carbonate phosphate, as already observed in our previous studies [14]. In fact, already in the unprocessed spectra (Fig. 1d), the main band around 1020 cm^{-1} related to the asymmetric stretching mode of PO_4^{3-} and the signals around 1460–1410 cm^{-1} and 872 cm^{-1} typical of vibrational modes of the CO_3^{-2} group can be easily distinguished.

These data are of interest considering a previous study suggesting that ovarian cancer cells switch to a calcifying phenotype and express bone related transcription factors and bone matrix proteins to cause the calcification deposition [18]. Moreover, the influence of female reproductive apparatus was considered by Das and colleagues who affirmed that the formation of calcifications may be linked to the secretion of collagen and could also be affected by hormones [12].

This work investigated the possibility of exploiting the biochemical information contained in microcalcifications observed in different tissues, to understand the aggressiveness of ovarian cancer and its potential progression in borderline patients. This information might also support pathologists in differentiating borderline tumors from carcinoma especially when the invasive component is limited. In fact, the ESMO–ESGO consensus conference recommendations on ovarian cancer reports that microinvasion (<5 mm) can be seen in borderline tumors but these cases should still be regarded as borderline for classification and management purposes [19].

Principal component analysis (PCA) was performed on spectral data of all tissue samples analyzed (**1-bl**, **2-bl**, **3-bl**, **lg** and **hg**) after applying the second derivative to the spectra recorded following the procedure shown in Fig. 1. Second derivative highlights smaller spectral differences among the spectra of the samples. In fact, it enhances the gradients of the spectral bands of interest with respect to the baseline and allows resolving overlapped peaks.

PCA was applied on spectral data in the region 800–1500 cm^{-1}, where signals of amorphous calcium carbonate phosphate, which is the main substance in PBs, are observed. The resulting score plot PC1 *vs* PC2 is reported in Fig. 2a, and interesting chemical similarities and dissimilarities among the samples can be observed. Meanwhile, the score plot for PC3 *vs* PC4 showed no discrimination (Fig. S3b).

Considering PC1 and PC2, the explained variance was not very high, and 20 PCs would be needed to reach 80 % (Scree plot in Fig. S3a). However, PC1 and PC2 were informative, which can be supported by analyzing the corresponding loadings (Fig. 2b). PCA loadings represent the variance in the wavenumber directions. They are used to identify spectral signals with a high degree of relevance for the observed pattern in the distribution of scores. By considering the loadings plot associated with PC1 and PC2 (Fig. 2b), the most discriminant wavenumbers are the

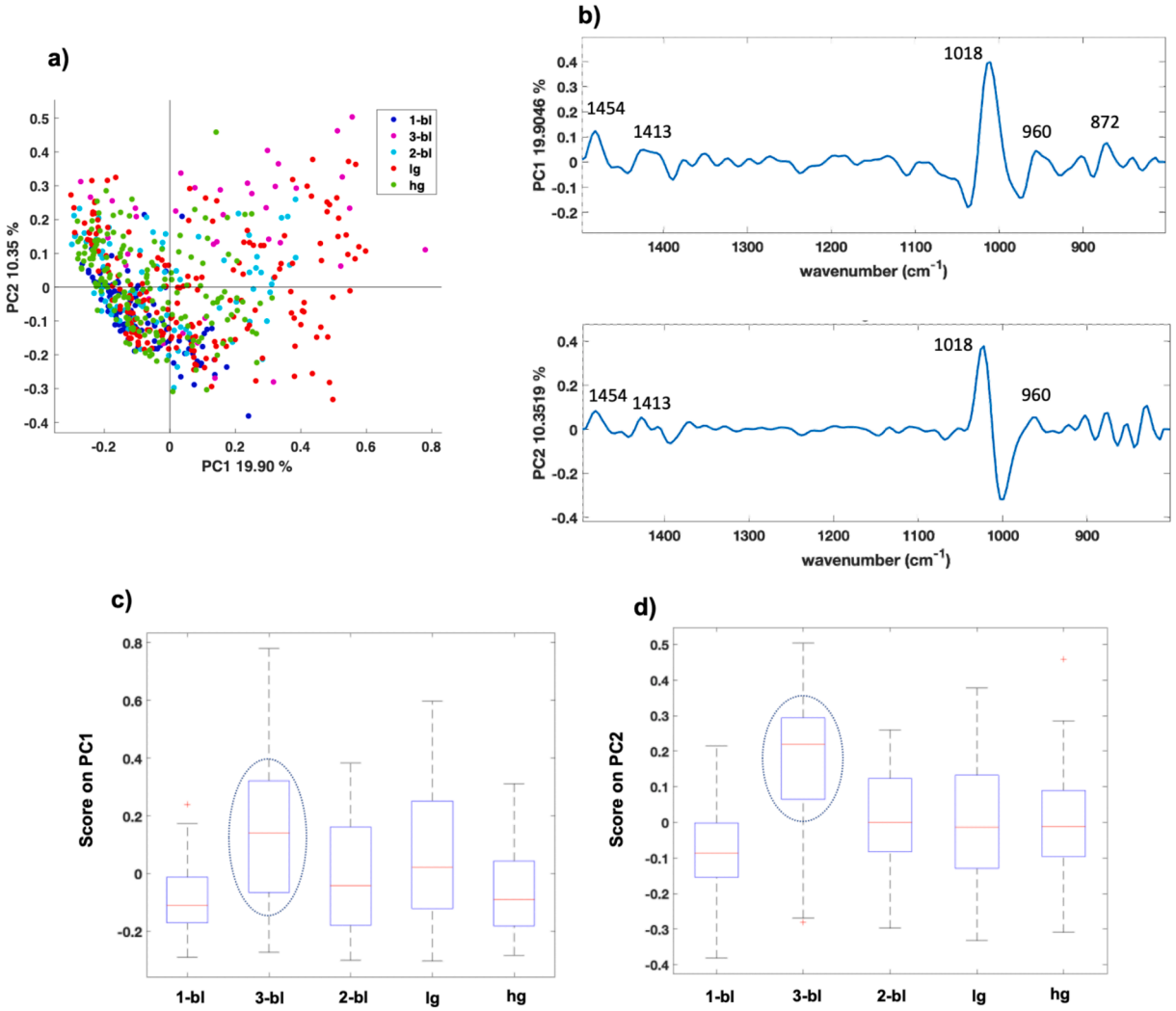

Fig. 2. (a) Score plot PC1 *vs* PC2 for microcalcifications from borderline patients (**1-bl**, **2-bl** and **3-bl**), high-grade patients (**hg**) and low-grade patients (**lg**); (b) Loadings plots related to PC1 (top) and PC2 (bottom) (c) box-plots of PC1 scores; (d) box-plots of PC2 scores.

signals at 872, 960, 1018, 1413, and 1454 cm^{-1} related to the carbonate and phosphate anions present in PBs. This result suggests that the different carbonate and phosphate content in the various samples accounts for their differentiation in the score plot PC1 *vs* PC2.

In detail, from the score plot PC1 *vs* PC2 (Fig. 2a) it can be seen that the spectra from the microcalcifications associated with the **3-bl** patient seem to differ from most of the other data. The spectra extracted from the microcalcifications of borderline **1-bl** and **2-bl** patients tend to form a single cluster with the spectra from the high-grade (**hg**). From this trend, the spectral data for low-grade microcalcifications differ slightly, showing greater variability.

To better identify and visualize the differences and similarities among spectra of microcalcifications box plots of PC1 and PC2 scores were used (Fig. 2c and d). The median line of the box plot related to the spectra of microcalcifications of patient **3-bl** tends to lie outside the box-plots associated with **hg**, **lg**, **1-bl** and **2-bl**. This highlights the difference in the biochemical content of microcalcifications associated with patient **3-bl** compared with all other patients examined. On the other hand, the microcalcifications present in borderline **1-bl** and **2-bl** patients appear chemically similar to those in high-grade and low-grade patients.

Further investigation was carried out on the samples of the three borderline patients (**1-bl**, **2-bl**, **3-bl**) and the samples of the high-grade patients (**hg**). In fact, the finding of similarity or chemical diversity between the PBs of the borderline patients and those of the high-grade patients can be a crucial information for determining the evolution of the borderline case a priori.

For this purpose, PCA analysis was performed separately considering the spectral data of each borderline patient and all spectral data of microcalcifications of high-grade patients in the region 800–1500 cm^{-1}.

The score plot PC1 *vs* PC2 (Fig. 3a) shows that borderline **3-bl** microcalcifications are sufficiently discriminated on PC1 from the high-grade microcalcifications. However, such discrimination is not evident for the spectral data from the **1-bl** and **2-bl** microcalcifications (score plots **3b** and **3c**).

Regarding the loadings associated with PC1 and PC2 (Fig. S4), again it is confirmed that the discriminant wavenumbers are those related to carbonate and phosphate signals.

These results are further verified and shown using box plots of PC1 scores in Fig. 3(d–f) and PC2 scores in Fig. S5. In fact, in Fig. 3f the median line of the box plot related to the spectra of microcalcifications of patient **3-bl** is outside the box-plot of **hg** whereas for **1-bl** (Fig. 3d) and **2-bl** (Fig. 3e) compared to **hg** this divergence is not observed.

When PCA analysis was performed, between the spectral data of each individual borderline patient, and the spectral data of the microcalcifications of all samples from the low-grade patients, no clear discrimination was observed (Fig. S6). This is probably due to the higher variability of the data for low-grade tumors, as it can be seen from the box and whiskers in plots **2b** and **2c**.

To verify whether the biochemical differences among samples can be attributed to carbonate and phosphate content as identified by loadings, a comparison of the average spectra of the microcalcifications of the borderline patients (**1-bl**, **2-bl** and **3-bl)** and those of **hg** and **lg** was performed (Fig. 4a). Pre-processing applied to the spectral data was a baseline correction technique. In this way, the spectra maintained on the y-axis scale the absorbance intensity values correlated with the abundance of the chemical species associated with the IR signal.

The region of the spectrum analyzed was 800–1550 cm^{-1}. This range includes the characteristic signals of amorphous calcium carbonate phosphate. In fact, as can be seen in Fig. 4a, the band at 1018 cm^{-1} is related to ν_3 PO_4^{3-} asymmetric stretching mode and the shoulder around 960 cm^{-1}, assigned to ν_1 PO_4^{3-} symmetric stretching mode, is a fingerprint confirming the structure of the amorphous calcium carbonate phosphate. The signals at 1454, 1413 cm^{-1} were assigned to ν_3 CO_3^{-2} asymmetric stretching modes while 872 cm^{-1} is associated with ν_2 out-of-plane vibration of CO_3^{-2}.

By comparing the average spectra obtained from the microcalcifications in the different samples analyzed, it is evident that the peak intensity at 1018 cm^{-1} in **3-bl** sample is lower than that in **hg** and in **1-bl** and **2-bl** samples, revealing a reduced phosphate content. Meanwhile, the average spectra of **1-bl** and **2-bl** show peak intensities similar to each other and, in some spectral regions, closer to those of the **hg**. These results confirm those obtained by PCA.

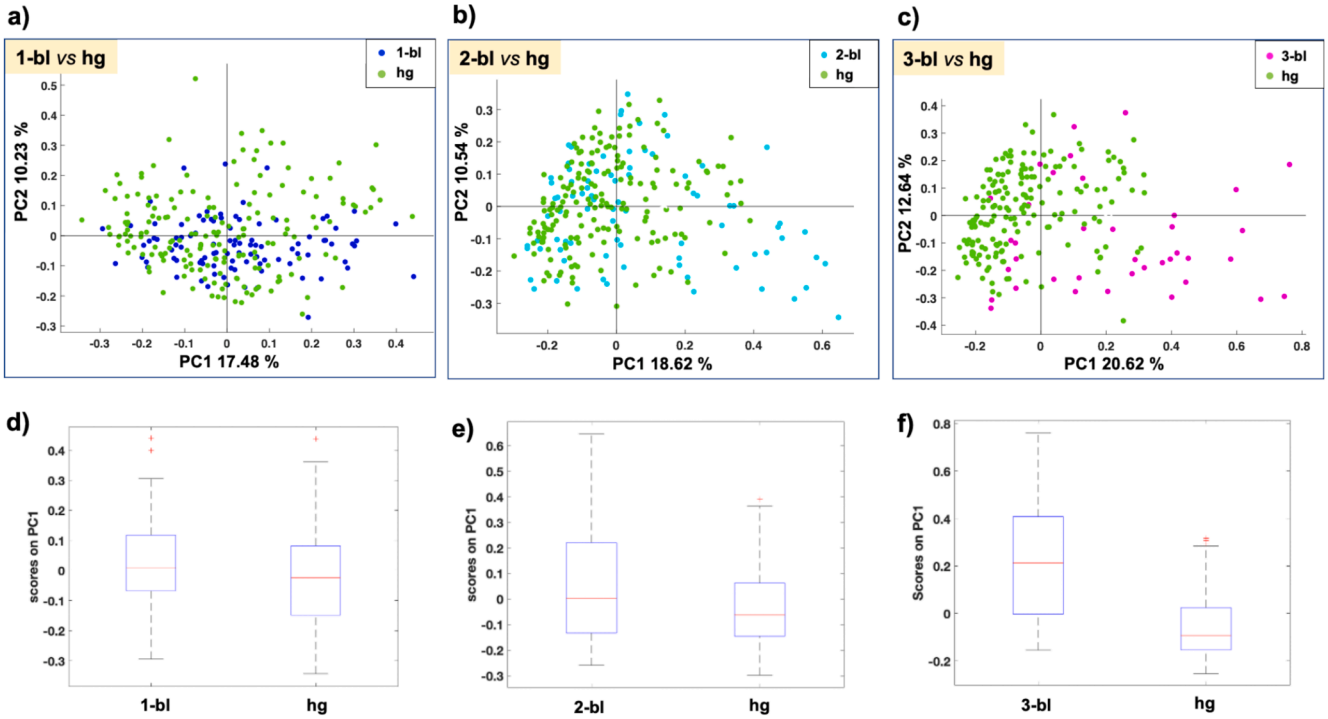

Fig. 3. Score plots PC1 *vs* PC2 for microcalcifications from borderline and high-grade patients: **1-bl** and **hg** (a), **2-bl** and **hg** (b), **3-bl** and **hg** (c). Box-plots of PC1 scores for microcalcifications from borderline and high-grade patients: **1-bl** and **hg** (d), **2-bl** and **hg** (e), **3-bl** and **hg** (f).

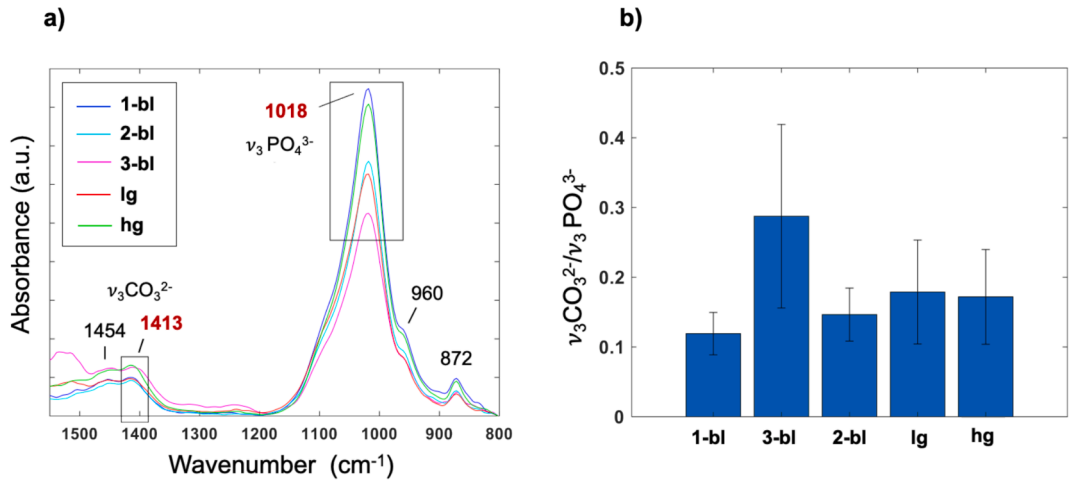

Fig. 4. (a) The averaged spectra of the microcalcifications of borderlines (**1-bl**, **2-bl** and **3-bl**), high-grade tumors (**hg**) and low-grade tumors (**lg**); (b) mean ratio of signal absorbances related to CO_3^{2-} (1413 cm^{-1}) and PO_4^{3-} (1018 cm^{-1}) from the spectra of microcalcifications in the borderline (**1-bl**, **2-bl** and **3-bl**), high-grade tumors (**hg**) and low-grade tumors (**lg**).

Recent studies on microcalcifications present in breast tumors have shown that carbonate amount may be related to the aggressiveness of the disease [20–22], specifically, carbonate level was found to be decreasing in progressively more invasive tumors [23].

Given these findings regarding microcalcifications in breast cancer, this work investigated the carbonate content in microcalcifications found in the three borderline cases and those present in patients with high-grade and low-grade cancer.

The absorbance ratio of CO_3^{2-} and PO_4^{3-} signals was used to estimate carbonate levels. The value of the CO_3^{2-}/PO_4^{3-} ratio turns out to be the higher the carbonate content. The signal at 1018 cm^{-1} was chosen to obtain the maximum absorbance of the phosphate group, while the signal at 1413 cm^{-1} was selected for the carbonate group (Fig. 3a). All carbonate signals show an increment in intensity as carbonate substitution increases, but this increase is more easily seen for bands around 1400 and 1450 cm^{-1} [21]. Therefore, the ratio of peak intensity at 1413 cm^{-1} to the peak intensity at 1018 cm^{-1} (I_{1413}/I_{1018}) was determined to assess the carbonate level in the various microcalcifications.

It has been observed that the carbonate content is significantly different among the three borderline patients (**1-bl**, **2-bl,** and **3-bl**) (Fig. 4b). In addition, in the borderline **3-bl** patient, the amount of carbonate is noticeably higher than in the other borderline patients **1-bl** and **2-bl** and also with respect to the **lg** to **hg** samples. While in the **lg** and **hg** the level of carbonate is similar. This outcome on similarity and dissimilarities in chemical composition of microcalcifications is in agreement with spectral data analysis performed with PCA and box plot (Fig. 2 and Fig. 3).

Taking into consideration studies related to breast cancer microcalcifications, according to which a higher level of carbonates indicates a lower aggressiveness, these results suggest that the borderline **3-bl** tumor is less aggressive than **1-bl** and **2-bl** tumors (Fig. 4b).

This hypothesis is strongly supported by the TNM staging (Table 1), where case **3-bl** is the only borderline tumor classified as pT1a while **1-bl** and **2-bl** are respectively pT2a and pT3b. In addition, both immunohistochemistry for BRAFV600E mutant protein and molecular analysis for BRAF gene showed BRAFV600E mutation in case **3-bl** (Fig. 5), while resulted wild type in the other two cases (**1-bl** and **2-bl**). Immunohistochemistry (IHC) using mutation-specific antibodies against BRAFV600E provides an alternative inexpensive method for the rapid identification of BRAFV600E mutation-positive tumors. IHC for BRAFV600E is approved to be of value for clinical management of malignant neoplasms [24]. In our case, the hot spot mutation BRAFV600E was confirmed by PCR, performed in another Institution.

BRAFV600E mutated ovarian serous borderline tumors have been reported to be at low risk for progression to serous carcinoma [25]. Since evaluating of BRAFV600E mutational status was proposed as a potential tool for clinical management of ovarian serous borderline tumors, we might affirm that FTIR analysis has the same value in identifying low-risk borderline tumors but requiring minimal resources and giving faster results. This prognostic approach might also improve inter-observer variability among pathologists in the setting of borderline tumors, as previously suggested for the use of immunohistochemistry [26].

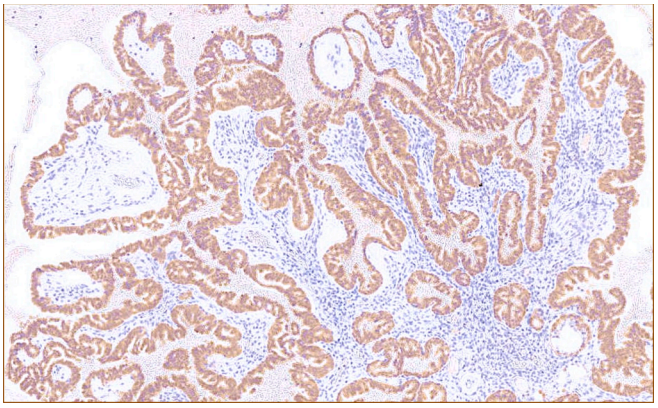

Fig. 5. Immunohistochemistry using mutation-specific antibodies against BRAFV600E mutated protein on paraffin section from case (**3-bl**). Positive reaction is evident in the cytoplasm of the epithelial neoplastic cells (brown color), hematoxylin counterstained, low power field.

Therefore, if a larger court of patients confirms the preliminary results obtained, the Micro-FTIR analysis may represent a complementary tool for histological diagnosis with implication for predicting the risk for tumor progression. This approach also opens a new insight in the cytological evaluation of pelvic washing. In such samples, the presence of psammoma bodies was reported in 3.6 % of cases, including serous ovarian tumors [27,28]. In these cases, FTIR should complement morphological assessment in determining the nature of underlying processes.

4. Conclusions

This work investigated the chemical composition of psammoma bodies, microcalcifications often observed in serous epithelial ovarian

cancer and serous borderline tumors, using FTIR spectroscopy. Unsupervised multivariate PCA analysis was applied to spectral data recorded in ATR mode from the microcalcifications in the tissues of three borderline, three high-grade, and three low-grade tumors.

Based on the respective PBs composition, two of the borderline patients (**1-bl** and **2-bl**) and high-grade ovarian carcinoma ones form a chemically uniform group, from whom the third borderline patient (**3-bl**) differentiates. The differences in the carbonate levels found in psammoma bodies present in the cancer tissues of patients account for this classification. A higher CO_3^{2-} content was found in PBs of borderline patient **3-bl** compared to that in both microcalcifications of patients with high- and low-grade ovarian carcinoma. On the other hand, borderline patients **1-bl** and **2-bl** showed a carbonate content close to that of the microcalcifications present in malignant epithelial ovarian cancer. As reported in the literature for microcalcifications in breast cancers, it is worth noting that an increase in carbonate content correlates with lower tumor aggressiveness and vice versa. Thus, FTIR analysis of psammoma bodies seems able to differentiate the borderline tumors and to give indications about their aggressiveness. These hypotheses agreed with the TNM histopathological classification and the result of the molecular analyses for BRAFV600E performed on the three borderline tumors. These preliminary findings suggest that the FTIR spectroscopic technique is a promising and valuable tool for identifying low-risk borderline tumors, requiring minimal resources and providing faster results.

CRediT authorship contribution statement

Monica Orsini: Conceptualization, Validation, Investigation, Writing – original draft, Writing – review & editing, Supervision. **Francesco Porcelli:** Conceptualization, Validation, Investigation, Writing – original draft, Writing – review & editing. **Antonella Bianchi:** Investigation, Resources, Formal analysis. **Martina Verri:** Investigation, Resources, Formal analysis. **Serena De Santis:** Investigation, Resources, Formal analysis, Writing – original draft, Writing – review & editing. **Giovanni Sotgiu:** Investigation, Resources, Formal analysis, Writing – review & editing. **Susanna Romano:** Investigation, Formal analysis. **Anna Crescenzi:** Conceptualization, Validation, Investigation, Writing – original draft, Writing – review & editing.

Funding

This research received no external funding.

Declaration of competing interest

The authors declare that they have no known competing financial interests or personal relationships that could have appeared to influence the work reported in this paper.

Appendix A. Supplementary data

Supplementary data to this article can be found online at https://doi.org/10.1016/j.saa.2024.125301.

Data availability

Data will be made available on request.

References

[1] R.L. Siegel, K.D. Miller, H.E. Fuchs, A. Jemal, Cancer statistics, CA Cancer J. Clin. 72 (2022) (2022) 7–33, https://doi.org/10.3322/caac.21708.
[2] A.K. Höhn, C.E. Brambs, G.G.R. Hiller, D. May, E. Schmoeckel, L.-C. Horn, WHO Classification of Female Genital Tumors, Geburtshilfe Frauenheilkd. 81 (2021) (2020) 1145–1153, https://doi.org/10.1055/a-1545-4279.
[3] A. González-Martín, P. Harter, A. Leary, D. Lorusso, R.E. Miller, B. Pothuri, I. Ray-Coquard, D.S.P. Tan, E. Bellet, A. Oaknin, J.A. Ledermann, Newly diagnosed and relapsed epithelial ovarian cancer: ESMO Clinical Practice Guideline for diagnosis, treatment and follow-up, Ann. Oncol. 34 (2023) 833–848, https://doi.org/10.1016/j.annonc.2023.07.011.
[4] N. Bourdel, C. Huchon, C. Abdel Wahab, H. Azaïs, S. Bendifallah, P.-A. Bolze, J.-L. Brun, G. Canlorbe, P. Chauvet, E. Chereau, B. Courbiere, T. De La Motte Rouge, M. Devouassoux-Shisheboran, C. Eymerit-Morin, R. Fauvet, E. Gauroy, T. Gauthier, M. Grynberg, M. Koskas, E. Larouzee, L. Lecointre, J. Levêque, F. Margueritte, E. D'argent Mathieu, K. Nyangoh-Timoh, L. Ouldamer, J. Raad, E. Raimond, R. Ramanah, L. Rolland, P. Rousset, C. Rousset-Jablonski, I. Thomassin-Naggara, C. Uzan, M. Zilliox, E. Daraï, Borderline ovarian tumors: French guidelines from the CNGOF. Part 2. Surgical management, follow-up, hormone replacement therapy, fertility management and preservation, J. Gynecol. Obstet. Hum. Reprod. 50 (2021) 101966, https://doi.org/10.1016/j.jogoh.2020.101966.
[5] Z. Movasaghi, S. Rehman, I. ur Rehman, Fourier transform infrared (FTIR) spectroscopy of biological tissues, Appl. Spectrosc. Rev. 43 (2008) 134–179, https://doi.org/10.1080/05704920701829043.
[6] M.J. Baker, J. Trevisan, P. Bassan, R. Bhargava, H.J. Butler, K.M. Dorling, P. R. Fielden, S.W. Fogarty, N.J. Fullwood, K.A. Heys, C. Hughes, P. Lasch, P. L. Martin-Hirsch, B. Obinaju, G.D. Sockalingum, J. Sulé-Suso, R.J. Strong, M. J. Walsh, B.R. Wood, P. Gardner, F.L. Martin, Using Fourier transform IR spectroscopy to analyze biological materials, Nat. Protoc. 9 (2014) 1771–1791, https://doi.org/10.1038/nprot.2014.110.
[7] A. Zancla, S. De Santis, G. Sotgiu, C. Taffon, A. Crescenzi, M. Orsini, Micro-FTIR spectroscopy as robust tool for psammoma bodies detection in papillary thyroid carcinoma, Spectrochim. Acta A Mol. Biomol. Spectrosc. 229 (2020) 117984, https://doi.org/10.1016/j.saa.2019.117984.
[8] S. De Santis, F. Porcelli, G. Sotgiu, A. Crescenzi, A. Ceccucci, M. Verri, M. Caricato, C. Taffon, M. Orsini, Identification of remodeled collagen fibers in tumor stroma by FTIR Micro-spectroscopy: a new approach to recognize the colon carcinoma, Biochim. Biophys. Acta (BBA) – Mol. Basis Dis. 1868 (2022) 166279. https://doi.org/10.1016/j.bbadis.2021.166279.
[9] L. Li, J. Wu, L. Yang, H. Wang, Y. Xu, K. Shen, Fourier transform infrared spectroscopy: an innovative method for the diagnosis of ovarian cancer, Cancer Manag. Res. 13 (2021) 2389–2399, https://doi.org/10.2147/CMAR.S291906.
[10] L. Li, X. Bi, H. Sun, S. Liu, M. Yu, Y. Zhang, S. Weng, L. Yang, Y. Bao, J. Wu, Y. Xu, K. Shen, Characterization of ovarian cancer cells and tissues by Fourier transform infrared spectroscopy, J. Ovarian Res. 11 (2018) 64, https://doi.org/10.1186/s13048-018-0434-8.
[11] P. Stec, J. Dudała, A. Wandzilak, P. Wróbel, Ł. Chmura, M. Szczerbowska-Boruchowska, Fourier transform infrared microspectroscopy analysis of ovarian cancerous tissues in paraffin and deparaffinized tissue samples, Spectrochim. Acta A Mol. Biomol. Spectrosc. 297 (2023) 122717, https://doi.org/10.1016/j.saa.2023.122717.
[12] D.K. Das, Psammoma body: A product of dystrophic calcification or of a biologically active process that aims at limiting the growth and spread of tumor? Diagn. Cytopathol. 37 (2009) 534–541, https://doi.org/10.1002/dc.21081.
[13] R. Bonfiglio, A. Granaglia, R. Giocondo, M. Scimeca, E. Bonanno, Molecular aspects and prognostic significance of microcalcifications in human pathology: a narrative review, Int. J. Mol. Sci. 22 (2020) 120, https://doi.org/10.3390/ijms22010120.
[14] F. Porcelli, M. Verri, S. De Santis, A. Crescenzi, A. Bianchi, A.C. Felici, G. Sotgiu, S. Romano, M. Orsini, Considerations on chemical composition of psammoma bodies: automated detection strategy by infrared microspectroscopy in ovarian and thyroid cancer tissues, Spectrochim. Acta A Mol. Biomol. Spectrosc. 298 (2023) 122792, https://doi.org/10.1016/j.saa.2023.122792.
[15] S. De Santis, G. Sotgiu, A. Crescenzi, C. Taffon, A.C. Felici, M. Orsini, On the chemical composition of psammoma bodies microcalcifications in thyroid cancer tissues, J. Pharm. Biomed. Anal. 190 (2020) 113534, https://doi.org/10.1016/j.jpba.2020.113534.
[16] A. Vinceova, B. Ch, Annals of Clinical and Medical Case Reports Borderline Ovarian Tumors-Definition and Classification, (2024). https://acmcasereport.org/.
[17] M.B. Amin, F.L. Greene, S.B. Edge, C.C. Compton, J.E. Gershenwald, R.K. Brookland, L. Meyer, D.M. Gress, D.R. Byrd, D.P. Winchester, The Eighth Edition <scp>AJCC</scp> Cancer Staging Manual: Continuing to build a bridge from a population-based to a more "personalized" approach to cancer staging, CA Cancer J. Clin. 67 (2017) 93–99. https://doi.org/10.3322/caac.21388.
[18] J. Wen, Z. Zhao, L. Huang, L. Li, J. Li, Y. Zeng, J. Wu, Y. Miao, Switch of the ovarian cancer cell to a calcifying phenotype in the calcification of ovarian cancer, J. Cancer 9 (2018) 1006–1016, https://doi.org/10.7150/jca.22932.
[19] N. Colombo, C. Sessa, A. du Bois, J. Ledermann, W.G. McCluggage, I. McNeish, P. Morice, S. Pignata, I. Ray-Coquard, I. Vergote, T. Baert, I. Belaroussi, A. Dashora, S. Olbrecht, F. Planchamp, D. Querleu, T. Baert, S. Banerjee, I. Belaroussi, P. Blecharz, I. Bruchim, D. Cibula, N. Colombo, N. Concin, B. Davidson, A. Dashora, M. Devouassoux-Shisheboran, A. du Bois, A. Ferrero, R. Glasspool, A. González-Martin, V. Heinzelmann-Schwarz, F. Joly, J.W. Kim, F. Kridelka, J. Ledermann, D. Lorusso, S. Mahner, W.G. McCluggage, I. McNeish, M. Mikami, M.R. Mirza, P. Morice, S. Nicum, S. Olbrecht, D.M. O'Donnell, P. Pautier, F. Planchamp, S. Pignata, D. Querleu, I. Ray-Coquard, A. Rodolakis, J. Sehouli, F. Selcukbiricik, C. Sessa, N. Singh, D.S.P. Tan, D. Timmerman, G. Tognon, J. van der Velden, I. Vergote, P.O. Witteveen, A.G. Zeimet, ESMO–ESGO consensus conference recommendations on ovarian cancer: pathology and molecular biology, early and advanced stages, borderline tumours and recurrent disease, Ann. Oncol. 30 (2019) 672–705, https://doi.org/10.1093/annonc/mdz062.
[20] Y. Yang, Y. Yang, Z. Liu, L. Guo, S. Li, X. Sun, Z. Shao, M. Ji, Microcalcification-based tumor malignancy evaluation in fresh breast biopsies with hyperspectral

stimulated Raman scattering, Anal. Chem. 93 (2021) 6223–6231, https://doi.org/10.1021/acs.analchem.1c00522.
[21] R. Baker, K.D. Rogers, N. Shepherd, N. Stone, New relationships between breast microcalcifications and cancer, Br. J. Cancer 103 (2010) 1034–1039, https://doi.org/10.1038/sj.bjc.6605873.
[22] K.S. Shin, M. Laohajaratsang, S. Men, B. Figueroa, S.M. Dintzis, D. Fu, Quantitative chemical imaging of breast calcifications in association with neoplastic processes, Theranostics 10 (2020) 5865–5878, https://doi.org/10.7150/thno.43325.
[23] S. O'Grady, M.P. Morgan, Microcalcifications in breast cancer: From pathophysiology to diagnosis and prognosis, Biochim. Biophys. Acta (BBA) – Rev. Cancer 1869 (2018) 310–320, https://doi.org/10.1016/j.bbcan.2018.04.006.
[24] A. Crescenzi, Z. Baloch, Immunohistochemistry in the pathologic diagnosis and management of thyroid neoplasms, Front. Endocrinol. (Lausanne) 14 (2023), https://doi.org/10.3389/fendo.2023.1198099.
[25] M.H. Chui, S.K. Kjaer, K. Frederiksen, C.G. Hannibal, T.-L. Wang, R. Vang, I.-M. Shih, *BRAFV600E* -mutated ovarian serous borderline tumors are at relatively low risk for progression to serous carcinoma, Oncotarget 10 (2019) 6870–6878, https://doi.org/10.18632/oncotarget.27326.
[26] N. Missaoui, S. Salhi, A. Bdioui, S. Mestiri, N. Abdessayed, M. Mokni, M.T. Yacoubi, Immunohistochemical characterization improves the reproducibility of the histological diagnosis of ovarian carcinoma, Asian Pac. J. Cancer Prev. 19 (2018) 2545–2551, https://doi.org/10.22034/APJCP.2018.19.9.2545.
[27] E. Yamamoto, K. Warigaya, Y. Kinoshita, A. Yamamoto, S. Murata, Low-grade serous carcinoma detected from intraoperative peritoneal washings: cytological findings and detection of <scp>KRAS</scp> mutation, Cancer Rep. 5 (2022), https://doi.org/10.1002/cnr2.1676.
[28] T. Sun, M.B. Pitman, V.F. Torous, Determining the significance of psammoma bodies in pelvic washings: A 10-year retrospective review, Cancer Cytopathol. 129 (2021) 83–89, https://doi.org/10.1002/cncy.22346.